

## PDF hosted at the Radboud Repository of the Radboud University Nijmegen

The following full text is a publisher's version.

For additional information about this publication click this link.

<http://hdl.handle.net/2066/92718>

Please be advised that this information was generated on 2018-07-08 and may be subject to change.

RAMAN AND FAR INFRARED SPECTROSCOPY OF THE INCOMMENSURATE  
STRUCTURE  $\text{Na}_2\text{CO}_3$

H. NEEKIS, K. HANSEN, A. JANNER, T. JANSSEN and P. WYDER  
Faculty of Science, University of Nijmegen, Toernooiveld  
6525 ED Nijmegen, The Netherlands

Th. RASING  
Department of Physics, University of California, Berkeley,  
CA 94720, U.S.A.

**Abstract** The lattice vibrations of  $\text{Na}_2\text{CO}_3$  in the incommensurate phase have been studied by means of Raman and far infrared (F.I.R.) spectroscopy. The results exhibit strong temperature dependences which can be related to those of the modulation parameters.

INTRODUCTION

An incommensurate crystal structure is characterized by the fact that labelling of its diffraction pattern requires more than three (integer) indices. For a modulated structure this means that the period of the modulation is rationally independent of the underlying lattice periodicity. Therefore, incommensurate crystal structures do not have 3-dimensional space group symmetry. A clear indication of incommensurability is present if the modulation period varies continuously with respect to the other periods as a function of external parameters (temperature, pressure, etc.). Consequently, in that case a rational approximation is physically not meaningful.

$\text{Na}_2\text{CO}_3$  in its  $\gamma$ -phase is an example of an incommensurate modulated structure with a strongly temperature dependent wave vector. This phase exists below  $T_1 = 620$  K. The modulation consists mainly of rotations of the  $\text{CO}_3^{2-}$  ions. De Pater<sup>1</sup> has reported a lock-in transition at  $T_2 = 120$  K. In the incommensurate phase, the modulation amplitude and both length and direction of the modulation wave vector vary with temperature. Therefore,  $\gamma\text{-Na}_2\text{CO}_3$  is well suited to study the effects of the modulation on the physical properties of incommensurate crystal structures.

EXPERIMENTAL

The crystals were grown in a platinum crucible, using the Bridgman method, thus polydomain samples with one preferred direction along the crucible were obtained.

For the F.I.R. transmission experiments, different thin plates were cut perpendicular to the above mentioned direction (presumably the  $c$ -axis), whereas transparent regions were chosen for the Raman scattering.

The F.I.R. measurements were done between 5 K and 300 K, in a He-cooled continuous flow cryostat with a Fourier transform interferometer. The light source was a medium pressure mercury lamp.

For the Raman experiments, the crystals were placed in a specially designed variable temperature cryostat, with working temperatures between 5 K and 700 K. An  $\text{Ar}^+$  Laser (514,5 nm) served as exciting radiation source. The scattered light was analysed at right angles with a double grating monochromator, after which the signal was recorded with the usual photon counting techniques. No polarization analyzer was used, because of the lack of single crystals.

SELECTION RULES

The selection rules for I.R. absorption and Raman scattering are closely related to the crystal symmetry. In the case of an incommensurate structure, the lack of translational symmetry prohibits the use of ordinary space groups. De Wolff<sup>2</sup> and Janner and Janssen<sup>3</sup> however, have shown that higher (3+d) dimensional so called superspacegroups can restore the translational symmetry for incommensurate structures. With the help of these superspacegroups, one can find the appropriate selection rules (Janssen<sup>4</sup>).

For the case of  $\text{Na}_2\text{CO}_3$  (superspacegroup  $P\frac{C_2}{1}^2/m$  in the incommensurate phase and spacegroup  $C2/m$  in the normal phase), the results can be found in Table 1.

TABLE I Number of modes in both phases, indicated as  $n_{\text{normal}}^{(\gamma)}$  +  $n_{\text{additional}}^{(\gamma)}$ ; vibrational and rotational modes only concern the  $\text{CO}_3^{2-}$  ions.

$C_{2h}$	$n_{\text{opt}}^{(\gamma)}$	$n_{\text{rot}}^{(\gamma)}$	$n_{\text{vibr}}^{(\gamma)}$	activity
$A_g$	4 + 5	1 + 4	4 + 4	Raman
$B_g$	2 + 10	2 + 2	2 + 8	Raman
$A_u$	3 + 10	2 + 2	2 + 8	I.R.
$B_u$	6 + 5	1 + 4	4 + 4	I.R.

EXPERIMENTAL RESULTS

Typical results of the measurements are the following.

F.I.R. Spectra

In Figure 1 a part of the low frequency F.I.R. spectrum is shown, together with the temperature dependence of the mode frequency (near  $50 \text{ cm}^{-1}$ ). For all modes observed, a shift with increasing temperature towards lower frequencies is seen. At temperatures above 300 K the transmission becomes too small for measurement. At 65 K there is a conspicuous change in the  $\omega(T)$  plot, which can also be seen in the width of the mode as a function of temperature. A comparable but less significant change in the slope of the  $\omega(T)$ -plot is seen at 120 K for another ( $\omega \approx 63 \text{ cm}^{-1}$ ) mode.

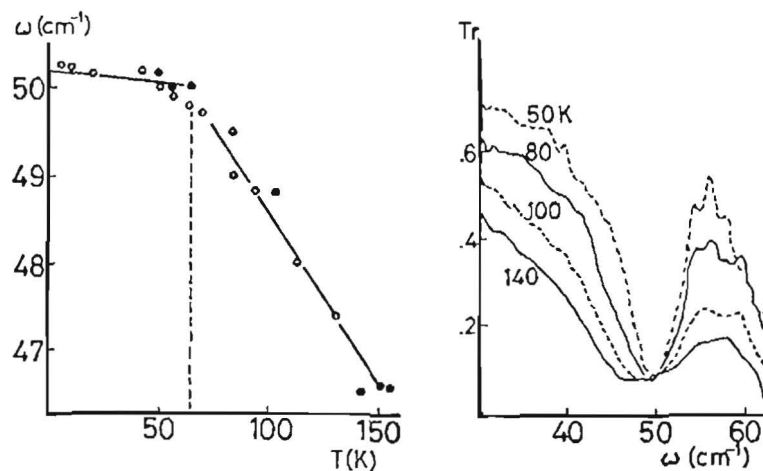


FIGURE 1 Left: Temperature dependence of the frequency of the mode near  $50 \text{ cm}^{-1}$ . Right: Low frequency F.I.R. transmission spectrum for various temperatures.

Raman Spectra

In Figures 2 and 3 some  $\omega(T)$  results are shown for the Raman measurements. A strong temperature dependence in particular at the highest temperatures can be seen for the external modes (figure 2). In fact many modes are ill-defined due to the large thermal broadening with increasing temperature. For the internal modes (two of which are plotted in figure 3), a less strong but never-

theless obvious temperature dependence is observed. All internal modes appear in pairs or even triples, the frequency difference for pairs tending towards zero on approaching  $T_1$ . The latter tendency is not observed for all internal modes.

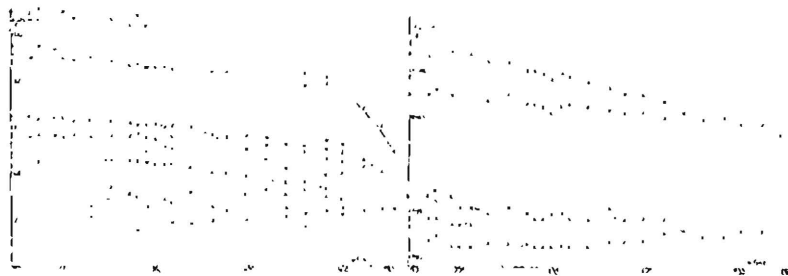


FIGURE 2 Raman shift vs. temperature for the low frequency external modes.

FIGURE 3 Raman shifts vs. temperature for the low frequency internal (vibrational) modes.

The strange and strong temperature dependence of many modes could be explained by the combined influence of the temperature dependence of the modulation wave vector and the amplitude. The connection between the two can be found by considering a harmonic oscillator model for an incommensurate system. This model, applied to  $\text{Rb}_2\text{ZnBr}_4$ , has been discussed in ref. 5. Summarizing, we have observed many modes with a strong temperature dependence. An explanation for these results is being worked on.

#### REFERENCES

1. G.J. de Pater and R.B. Helmholtz, *Phys. Rev.*, **B19**, 5735 (1979).
2. P.M. de Wolff, *Acta Cryst.*, **A33**, 493 (1977).
3. A. Janner and T. Janssen, *Phys. Rev.*, **B15**, 643 (1977), *Acta Cryst.*, **A36**, 399 (1980).
4. T. Janssen, *J. Phys. C: Solid State Phys.*, **12**, 5381 (1979).
5. Th. Rasing, P. Wyder and A. Janner, T. Janssen, *Phys. Rev.*, **B25**, 7504 (1982).

Acknowledgement - This work is part of the research program of the Stichting voor Fundamenteel Onderzoek der Materie (Foundation for Fundamental Research on Matter) and was made possible by financial support from the Nederlandse Organisatie voor Zuiver-Wetenschappelijk Onderzoek (Netherlands Organization for the Advancement of Pure Research).